CFD Modelling of the Electrical Phenomena and the Particle Precipitation Process of Wet ESP in Coaxial Wire-tube Configuration

S. Kaiser and H. Fahlenkamp
Department of Environmental Technology, Technical University of Dortmund, Germany

Abstract— Modelling the precipitation process in ESPs requires a strongly coupled system of the Maxwell-equations, describing the electrical conditions, and the Navier-Stokes-equations to determine the fluid flow. Another task is the implementation of the particle dynamics, i.e. the charging kinetic and the transformation of the Electric field distribution due to the resulting space charge. The objective of the presented work is the development of a CFD-based designing tool to predict the ESPs precipitation efficiency as a function of important parameters, such as the geometric patterns, electric potential, particle size distribution and concentration.

Keywords—Wet Electrostatic precipitation, Corona Quenching, numerical modelling

I. Introduction

The separation of dust- or aerosol-particles is mandatory in different kinds of industrial processes. Especially the sector of power generation requires efficient techniques for their removal, but applications of such techniques can also be found in other fields such as the production of cement and steel, in the fabrication of paper or in the petroleum industry. Under many operating conditions the electrostatic precipitation process can be used to achieve the required threshold for the emission of particles, while consuming a surprisingly low amount of energy. In modern power plants for example less than 0.1 % of the produced electrical power is necessary for the particle charging and precipitation. The efficiency of such devices is higher than 99 % [1]. Even though the first commercial use of this technology dates back to 1907 when F. Cottrell applied an Electrostatic Precipitator (ESP) to the collection of sulfuric acid mist and more than one hundred years of operational experience have gone by since then, the construction of ESP is still a difficult task for engineers based on a merely empirical approach [2].

The difficulties result from the fact, that the precipitation process is influenced by many different physical phenomena and therefore represents a very complex procedure. Since the fundamental relations to describe the process consist mainly of a set of partial differential equations, such as Navier-Stokes- and Maxwell-equations, the recent advances in modern numerical and computational techniques give rise to the opportunity of developing new concepts to properly design ESPs against the background of the main physical principles.

Thus the objective of the authors work is the creation of a computational model based on commercial software to provide a helpful tool for the construction and optimization of industrial ESP. Though the description of ESP processes with the aid of commercial CFD software is yet subject of different publications (e.g. [3, 4, 6, 14]), further attention is necessary to predict satisfactorily the behaviour of ESPs in different fields of application, especially if they have to deal with very high loads regarding the amount of fine particles. Thus in comparison to other publications this work is more focused on the effects caused by the particle space charge. The software ANSYS CFX®, which utilizes the numerical method known as “finite volumes”, is used to achieve this.

Corresponding author: Sven Kaiser
e-mail address: Sven.kaiser@bci.tu-dortmund.de

Presented at the 12th International Conference of Electrostatic Precipitation, ICESP, in May 2011 (Nuremberg, Germany)

II. Modelling environment

The presented numerical model is designed to operate on 3-dimensional coaxial wire-to-tube configurations. This kind of setup is mainly used in case of wet electrostatic precipitation processes, where the treated medium is saturated with water vapour (i.e. it has a relative humidity of 100 %). The particles being contained in the medium are treated as aerosols with a diameter distribution between 0.1 microns to 10 microns. Under these circumstances the precipitated particles at the collecting electrode are “washed off”, so they do not form a layer, which otherwise could significantly influence the distribution of the electric field, due to its higher electrical resistivity compared to the grounded electrode. Therefore it is possible to assume independency from time and thus utilize a steady state approach to describe the process. Furthermore the examination of liquid droplets (i.e. aerosols) justifies the assumption that particles, once they have reached the collecting electrode, are separated from the system and will not re-enter the fluid flow by any means.

It is generally believed that the resulting electrohydrodynamic-flow-field depends on the conditions at the inlet and outlet of the precipitation area [3]. Therefore two additional domains up- and downstream of the main volume are considered which do not contain a corona wire and possess electrically isolated walls. However, in accordance to [18] we found that, because of the circular geometry used in this study,

the influence of the secondary flow field induced by the electric forces (i.e. the electric wind) on the precipitation efficiency is negligible. This is in contrast to other electrode arrangements such as wire-to-plate configurations. Due to the high symmetry (the corona-wire is positioned precisely in the center of the tube) recirculation zones are only developed near the inlet and the outlet in the parts of the tube with isolated walls, but not inside the precipitation zone. This would only be the case if the corona-wire has a position eccentric to the tube-center to a certain degree (as it probably would occur in reality). This is not further investigated in the present work but may be subject of future publications.

The calculations are performed in a multiphase approach. The fluid-phase and the ionic space charge are considered continuous and thus can be described with an eulerian approach, while the discrete phase is characterized using particle tracking (Lagrange method).

The *k-ε* model is used to describe the turbulence in the eulerian phase and buoyancy is activated to consider the additional gravitational forces. The ANSYS Emag® solver is used to solve the electrostatic submodel, at which a user subroutine and user defined functions are applied to assign the boundary condition of the space charge density distribution on the corona-wire in an iterative procedure and to calculate the superimposed motion of ions caused by the electric field. The calculations of the particle charging process and the Coulomb forces acting on particles are implemented in terms of two coupled subroutines.

To determine the particle space charge distribution a mixed eulerian-lagrangian method similar to the one proposed by Gallimberti [16] is used.

A. Numerical modelling

The description of the electrohydrodynamic flow field is governed by a coupled system of Navier-Stokes-equations and Maxwell-equations. The connection between the two phenomena, the fluid flow on the one hand and the electrostatics on the other hand, is the charge density, because it contributes to the Poisson equation and the current continuity equation as well as to the momentum balance for the fluid flow. The space charge density itself is a source of electric potential and for this reason it is part of the Poisson equation and thus also determines the electric field distribution represented by the negative gradient of the potential.

$$\nabla^2 \Phi = -\frac{\rho}{\varepsilon_0} \qquad (1)$$

$$\vec{E} = -\nabla \Phi \qquad (2)$$

where Φ is the electric potential, ρ the space charge density, ε_0 the dielectric permittivity of free space and $\vec{E}$ the electric field.

According to many different authors the effect of the electric forces on the flow field, i.e. the electric wind can be modeled by including an additional source term $\vec{S}$ in the momentum balance which only depends on the space charge density and the strength of the electric field [4, 10].

$$\vec{S} = \vec{E} \cdot \rho \qquad (3)$$

The distribution of the space charge arises from the superposition of the proportions of the ionic space charge and the particle space charge, i.e. the free ions and the ones bounded to particles.

To calculate the ionic space charge distribution ρ_{ion} it is assumed that a certain amount of ions is generated in the active zone around the corona wire and than gets transported towards the collecting electrode where the ions leave the system. Under the assumption that the electric field strength at the surface of the corona corresponds to the breakdown electric field strength according to Peek´s formula [5] the amount of ions, which is injected at the wire surface, can be calculated in an iterative procedure so that the above condition is satisfied, as stated by different authors [6, 7, 8]. With the additional assumption of a homogeneous electric field inside the active corona zone the radial expansion (i.e. the position of the corona surface) can be determined as the intersection point of the undisturbed electric potential distribution (i.e. the Laplace-equation) and a straight line with the slope of the onset electric field strength. This procedure is described in detail by Gallimberti [17].

The ionic motion in the drifting zone is clearly dominated by the influence of the electric field and therefore can be described by applying a slip velocity $\vec{v}_{ion}$ between the ionic component and the uncharged component of the fluid.

$$\overrightarrow{v_{ion}} = b_{ion} \cdot \vec{E} \qquad (4)$$

where $\vec{E}$ is the electric field and b_{ion} is the mobility of ions which is a material property (more on the calculation of the ion mobility can be found in [13, 14]). In that way the velocity field, derived from the Navier-Stokes-equation, as well as the electric force are taken into account. Therefore it is possible to study the influence of the boundary conditions on the ionic space charge distribution of both aspects, the hydrodynamic, such as the inlet velocity and the turbulent dispersion on one hand and the electrical conditions, such as the applied voltage to the corona wire on the other hand.

In case of absence of particle space charge, the current density $\vec{j}$ can be calculated directly from the ionic space charge distribution since it is proportional to the concentration of ions.

$$\vec{j} = b_{ion} \cdot \rho_{ion} \cdot \vec{E} \qquad (5)$$

Furthermore the current continuity condition is valid.

$$\nabla \vec{j} = 0 \qquad (6)$$

So far the presented model (of the eulerian phase) is straightforward and corresponds to those of other authors [4, 7, 8, 15], though they mostly don't use commercial software to solve the problem. Differences arise if the phenomena caused by particle space charge are taken into account. To study the particle behavior and the precipitation efficiency as well as effects caused by the particle space charge, the particle dynamics, including the charging process and their motion, have to be modeled.

B. Particle dynamics

As already stated, particles are modeled using a lagrangian approach. To describe the charging process it has to be taken into account that the process depends on two different mechanisms, according to the particle size. Particles of a size lower than 1µm are mainly charged due to the diffusion charging mechanism, while in case of larger particles the field charging mechanism is dominant. As a modelling approach the field modified diffusion model derived by Lawless *et al*. [9] is adopted. The implementation is carried out in terms of an adsorption process, such as ions are removed from the eulerian phase and added to the lagrangian phase. The particle motion caused by the electric field force $\vec{F}_{elec}$ in that case only depends on the amount of charge accumulated on the particle q_{ion} and the local electric field in the surrounding of the particle $\vec{E}_p$.

$$\vec{F}_{elec} = q_{ion} \cdot \vec{E}_p \qquad (7)$$

This term is added to the momentum balance for each particle. The mutual interaction between the particle phase and the fluid flow is based on drag forces, which can be calculated by the Schiller-Naumann correlation [15].

Particles which collide with the grounded electrode, i.e. the inner wall of the outer tube are considered to be trapped, thus the precipitation efficiency can be determined by counting the trapped particles and than comparing the result with the particle size distribution at the inlet.

To indicate the functionality of the implemented charging mechanism the accumulation of particle charge with increasing particle traveling time, i.e. the charge accumulation along a particle trajectory, is shown in Fig. 1. As an example the charging kinetic of a particle of the size of 1 µm is shown. In addition the dashed line in the diagram represents the corresponding saturation charge. The saturation charge indicates the threshold of the field charging mechanism and is highly dependent of the local Electric field strength in the surrounding of the particle. Since the electric field in the drifting zone of the ESP is inhomogeneous, the saturation charge of a particle moving through this zone is also a function of the position of the particle and thus varies with the traveling time. As can be seen, the accumulated particle charge exceeds the saturation charge very quickly. This indicates the dominance of the diffusion charging mechanism for particles of the given size.

Due to the accumulated charge the particles experience an electrostatic deflection towards the inner wall of the tube where the precipitation takes place. By counting the particles of different size fractions arriving at the wall it is possible to determine the efficiency of the process. As an example the collection efficiency with respect to the particle size for two different applied voltages is shown in Fig. 2. The indicated curves represent the results of simulations in a testing geometry with a length of 1 m (excluding the inlet and outlet areas as stated before) and a diameter of 0.25 m. The corona electrode has a diameter of 1 mm and the inlet flow velocity is 1 m/s. The particles entering the geometry at the inlet are in a size range from 0.1 µm to 3 µm with a distribution equal in number per size fraction. Though this kind of distribution is of no significance in a nonacademic context it provides access to a facile comparison of the particle behavior for studying purposes. As expected, the collection efficiency increases with the particle diameter. Moreover it is not surprising that the curve representing the progression at the higher applied voltage, i.e. 35 kV, exhibits a shift towards higher values.

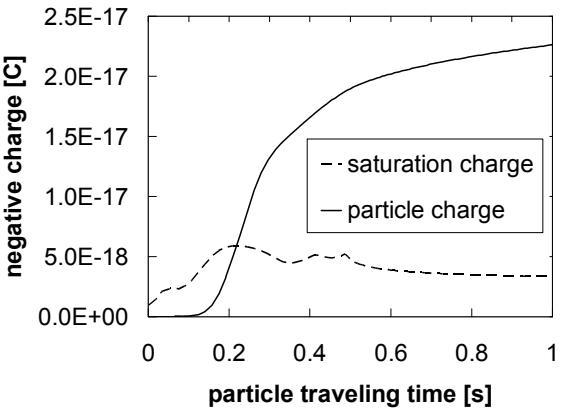

Fig. 1. Particle charge accumulation with time for a particle of the size of 1 µm. For comparison purpose the particle saturation charge due to the field charging mechanism is also illustrated.

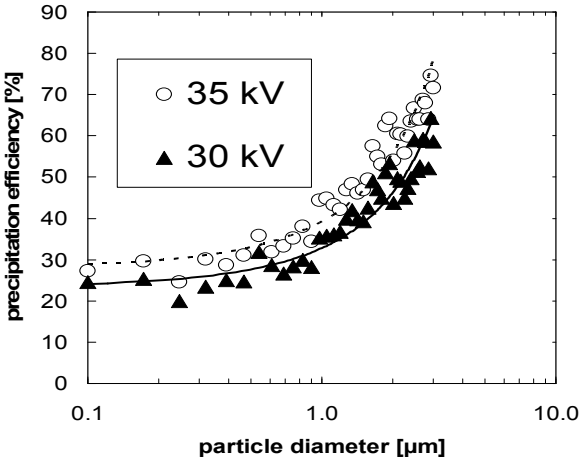

Fig. 2. Comparison of the computed precipitation efficiency for two different applied voltages.

Fig. 2 indicates that the general performance of ESPs is reflected well by the presented model.

To investigate the influence of the particle space charge, simulations with the same testing geometry and flow patterns as stated before are performed. A voltage of 25 kV is applied. The particle collective defined at the inlet consists of particles with a size range between 0.1 μm and 10 μm. The distribution is equal in number per size fraction and the overall particle load totals to a mass density of 3 mg particles per m3 fluid. This value is somewhat arbitrary chosen but it simply serves the purpose to study the influence of different particle loads on the distribution of the electric field.

The seed points of the particle trajectories at the inlet are equally spaced, i.e. they have a homogeneous distribution. Each trajectory represents a certain particle class (regarding the diameter) and, as long as a particle diameter distribution equal in number per size fraction is applied (as mentioned above), an equal amount of particles. The size fractions are allocated to the trajectories so that the particle density distribution is approximately constant along the radius. However, this is only valid at the inlet; since the radial distribution is highly altered along the axis of the tube due to the influence of the different migration velocities of each particle size fractions and the precipitation of particles.

In Fig. 3 the electric field strength is plotted against the distance from the corona wire in radial direction at three different points along the middle axis of the tube with a logarithmic scale regarding the ordinate. Position 1 is located near the inlet of the precipitation zone, position 2 is displaced towards the outlet of the tube and position 3 represents a location further downstream. The figure shows that the electric field is strongly influenced by the particle space charge. As expected, the shape of the radial electric field near the inlet, where the particle space charge is not yet significant, remains almost unaffected. In contrast it can be seen that the field strength at position 2 is raised near the collecting electrode. This effect comes along with a drop of the electric field strength near the wire, respectively at the surface of the corona, though the influence is still marginal. The weakening effect on the field strength near the wire becomes more noticeable at position 3 but it is still not comparable with the impact near the collecting electrode. Here the particles have accumulated a significant amount of charge and have drifted towards the collecting electrode. Because the electric field strength in the inner region of the drifting zone is much higher than in the outer regions and the particle drift velocity has the same general dependency, the particles tend to assemble near the tube wall (the radial expansion of the assembling zone decreases and gets closer to the wall along the tube). Therefore it is obvious that the particle space charge effect becomes more noticeable in this area.

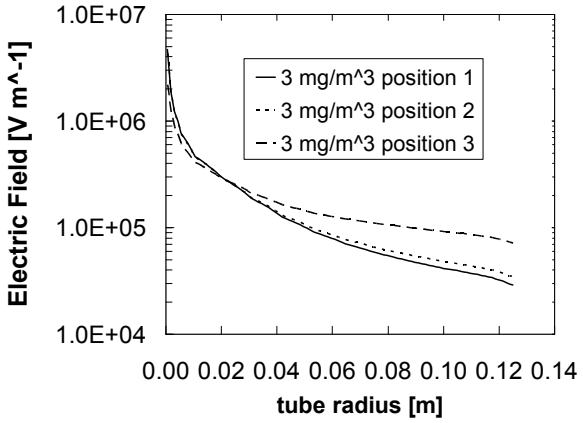

Fig. 3. Effect of particle space charge on the radial electric field at three different positions along the tube axis.

Fig. 4 shows a comparison between the electric field progressions at position 2 for two simulations with different particle loads. All other parameters are held constant and have the values stated before. In one case the particle load has a value of 10 mg per m^3 and the other case represents the one already mentioned before with a particle load of 3 mg per m^3

It is clear that the amount of particle space charge increases with the amount of particles and hence the difference between the two cases is apparent. The influence of the particle space charge is much higher in the outer region of the drifting zone as well as in the inner region near the wire for the case with a particle load of 10 mg per m^3. In the latter case the electric field strength at the surface of the corona is weakened significantly. Consequently it is assumed that under the given circumstances the effect known as corona quenching [11] would take place, resulting in a lower production rate of ions in the corona zone. This phenomenon is expected to be of great importance in case of high loads of very fine particles. The impact of the corona quenching effect on the current-voltage-characteristics of ESPs under these circumstances is therefore discussed in the following section.

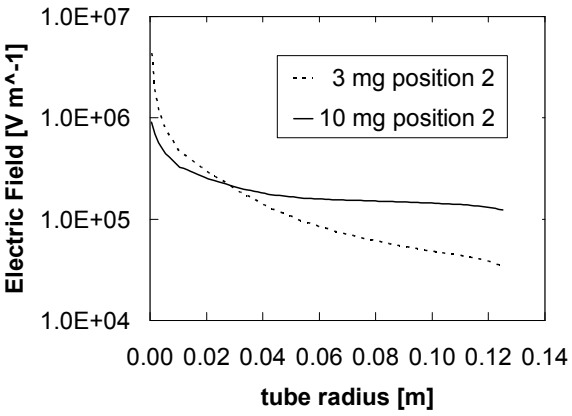

Fig. 4. Comparison between the effects of particle space charge on the radial electric field at two different particle loads at position 2.

III. CORONA QUENCHING EFFECT

For validation purpose it is desirable to compare the simulation results with data from the literature. Despite the fact that many authors have published their experimental and theoretical results regarding the present research topic it is difficult to find appropriate data. This is because a complete set of data is necessary to generate a valid CFD simulation, involving exact information about the geometry as well as extensive knowledge about the flow patterns, the electrical conditions and the properties of the deployed substances. In addition the majority of the published literature deals with wire to plate configurations. However some simulations with a setup based on experiments presented by Marquard *et al.* at the IX. International conference of electrostatic precipitation [12] are carried out. In the following the results of the simulations are compared with the reported measurements of Marquard *et al.* to investigate the functionality of the model.

The experimental ESP consists of a tube with a length of 30 cm and an inner diameter of 4 cm. The corona-wire has a diameter of 1 mm and approximately 10.8 m^3/h of air are flowing through it, at a temperature of 353 K. The highest applied voltage to the wire is about 9 kV. This value is significantly below the spark over voltage.

At first some simulations without particles are performed. The comparison between the computed and the measured current-voltage characteristics for this case is shown in Fig. 5. As can be seen in the figure, the results obtained from the CFD model are in a very good agreement with the measurements.

To investigate the influence of the particle space charge, simulations with the geometry based on the laboratory scale ESP of Marquard *et al.*, as described earlier in this section, are performed. The simulations are carried out with variable particle loads ranging from $5 \cdot 10^6$ to $3 \cdot 10^8$ # particles/cm^3 and different voltages. The particular parameters in each simulation are chosen in correspondence to the experiments published by this group.

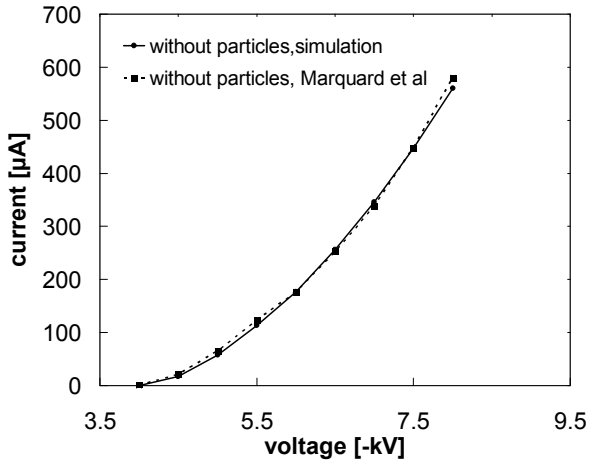

Fig. 5. Comparison of computed current-voltage-characteristic with data found in the literature [12].

As the particle phase SiO_2-aerosol is used, with a mean particle diameter of approximately 75 nm (log-normal distributed) and an electrical permittivity ε_r of 3.5. These small particle diameters make it necessary to implement some slight changes to the particle charging model to adopt it to this situation. The resulting current-voltage-characteristics of the simulations with particle loads of $3 \cdot 10^7$ # particles/cm^3 and $7 \cdot 10^7$ # particles/cm^3 are shown in Fig. 6 in comparison to the measured ones and the ones without particles. It can be seen that the higher the particle load the lower is the current at a given voltage, i.e. the curves are shifted towards lower values, in the measured curves as well as in the simulated ones. Obviously the agreement of the simulation- and measurement results is not as good as in case without particles. At low voltages (up to -6.5 kV) the current is underestimated. The reason for this may well be that in the calculation of the current the particle bounded charge arriving at the collecting electrode is neglected. This is indicated due to the fact that the deviations of the measured and simulated curves in this regime increase with growing particle loads (cp. Fig. 6) and the more particles are available the more particle bounded charge will contribute to the electric current.

At higher voltages the model overestimates the current. Moreover the simulated curves are nearly parallel to each other, unlike the measured ones. Because the current at the outer electrode is controlled by the amount of ions injected at the wire, the deviating behaviour of the simulated current-voltage-characteristics is basically caused by the applied corona-model. As described earlier in this paper, an approach based on the Laplace-equation is used to determine the location of the corona surface and this equation is independent of any space charge effects. That means though the numerical model accounts for the influence of the space charge on the potential distribution; it does not reflect the decrease of the radial corona expansion, i.e. the location of the corona surface is fixed throughout simulations with constant applied voltages to the wire.

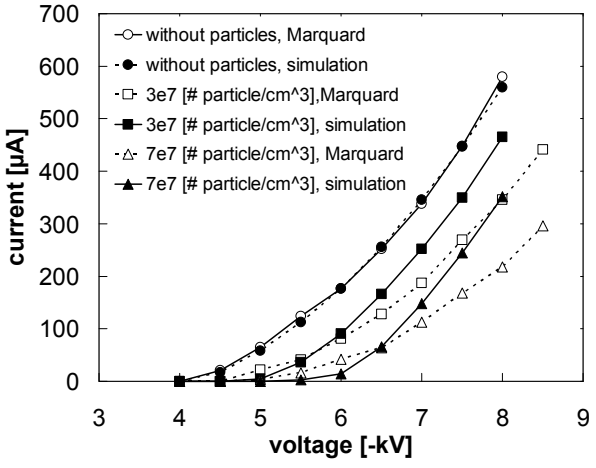

Fig. 6. Comparison of computed current-voltage-characteristics with data found in the literature [12] for a particle load of 3·107 # particles/cm3 and without particles.

Consequently the production of charge carriers is overestimated and the corona submodel acts similar to a shift in the onset electric field strength.

In Fig. 7 the computed precipitation efficiency of the process is plotted against the particle load and compared to the measured one. As can be seen the efficiency decreases with increasing particle loads. The driving force of the precipitation process is the Coulomb force, which depends on the particle charge and the electric field strength. The particles in the investigated size range are basically charged by the diffusion charging mechanism. In this case the charging process basically depends on the ion charge density in the surrounding of every particle. Since the ion charge density (and therefore the current) gets smaller with higher particle loads (as can be seen in Fig. 6) so does the charge on each particle. For example in the cases of particle loads of $3 \cdot 10^7$ # particles/cm^3 and $7 \cdot 10^7$ # particles/cm^3 with an applied voltage of -7 kV to the corona wire (see Fig. 7) a particle starting at the same point at the inlet has accumulated a charge of about $4.2 \cdot 10^{-18}$ C and $3.4 \cdot 10^{-18}$ C respectively after 0.15 seconds. The quotient of both values yields a result of approximately 1.2. On the other hand the quotient of the average value of the electric field (over the whole domain) of the same cases yields 1.05. This example shows that the decrease of the precipitation efficiency with growing particle loads is basically attributed to the differences in the particle charge.

Regarding the precipitation efficiency the general trend is reflected well by the model, even though the efficiency is slightly underestimated. This is caused by inaccuracies in the corona model as well as in the charging model. The underestimation of the efficiency signifies that the calculated charge on each particle is to small, since lower amounts of charge result in lower migration velocities. Taking into account, that the ionic space charge densities are overestimated by the corona model a better approximation would result in even lower values and this in turn would further reduce the computed efficiency.

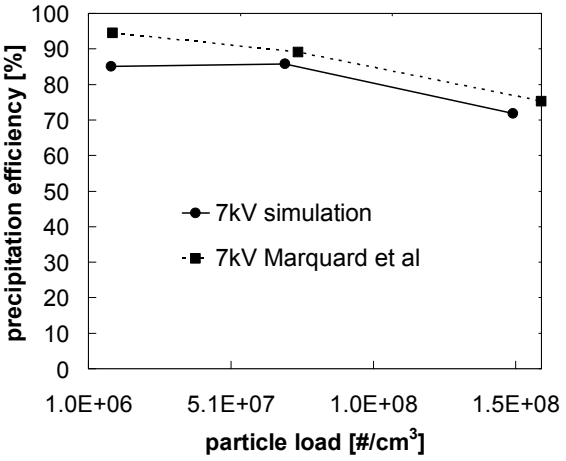

Fig. 7. Comparison of computed and measured precipitation efficiencies as a function of the particle load.

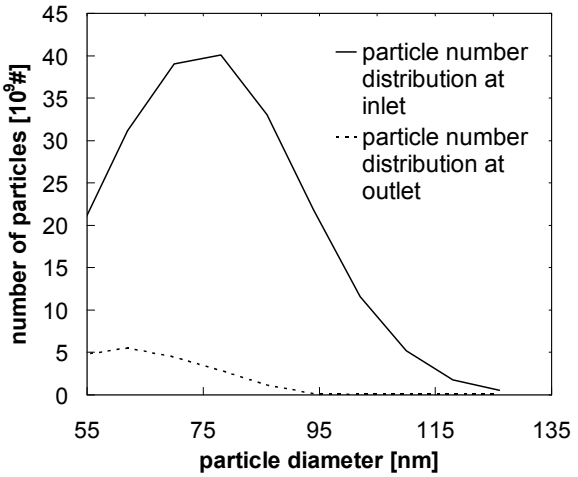

Fig. 8. Comparison of calculated particle size distributions at the inlet and the outlet of the laboratory scale ESP.

However, it should be stated that additional uncertainties arise from the experimental setup of Marquard. The measurements of particles only take place at the outlet of the precipitator but, as can be seen in Fig. 8, the calculated particle size distributions at the inlet and the outlet exhibit significant differences caused by the precipitation process. Since only the distribution at the outlet is known from the experiments it also has to be used as inlet distribution. Due to this, the overall particle number density and the mean particle diameter in the simulations tend to be underestimated

IV. Conclusion

The simulation performance of the presented CFD model shows the same tendencies as the measurements reported by Marquard *et al.* [12] and are also matching the considerations of other authors dealing with the given research topic. Especially regarding simulations with small particle loads reasonable results are yielded. This indicates that the behaviour of the model corresponds well to the observable physical effects in the wet electrostatic precipitation process even though deviations occur in the regime of corona quenching. The source of these deviations can be found basically in the used corona submodel, which is well established among the literature but does not reflect entirely the suppression of the corona due to the influence of the particle space charge. Therefore the corona submodel needs further development in conjunction with the calculation of the particle space charge distribution according to the computed particle motion to yield even better predictions of the general behaviour of wet ESPs.

Another substantial element of the model regarding the proper description of the corona quenching effect is the particle charging kinetics. Since the used "field modified diffusion model" is not originally designed to deal with particle sizes below 0.1 μm it is likely that the usage of other correlations will yield even better results regarding the simulation of such particles.

It is shown that simulating a coupled system of the electrical portions of the Maxwell-equations and the Navier-Stokes-equation with the ANSYS CFX® software leads to reasonable results. Moreover the used software package allows a comprehensive modelling of the ESP process. Compared to models such as the one of Gallimberti [16], which consists of a modular structure, the loss of comprehension is marginal if it occurs at all, since both models are based on similar assumptions and correlations, but due to the implementation of the model in commercially available software access for engineers to a useful tool for the design of wet ESPs could be provided easier in the future.

REFERENCES

[1] Theodore, L., Buonicore, A.J.; Air pollution control equipment; CRC Press Inc.;Boca Raton; 1988

[2] White,H.J.; Entstaubung industrieller Gase mit Elektrofiltern; VEB Deutscher Verlag für Grundstoffindustrie; Leipzig; 1969

[3] Schmid, H.-J.; Zum Partikeltransport in elektrischen Abscheidern; Dissertation; Universität Karlsruhe; 1998

[4] Lind, Leif; Nielsen, Niels F.; Simulation of particle transport in electrostatic precipitators; presented at the IX. International conference of electrostatic precipitation; A21-25 series; Kruger Gate,South Africa;2004; Available on homepage of ISESP: http://www.isesp.org

[5] Peek, F.W.; Dielectric Phenomena in High Voltage Engineering; McGraw Hill Book Co.;New York; 1929

[6] Nikas, K.S.P. *et al.*; Numerical simulation of the flow and the collection mechanism inside a laboratory scale electrostatic precipitator; Journal of Electrostatics 63;2005; p.423-443

[7] Anagnostopoulos, J. Bergeles, G.C., Corona discharge simulation in wire-duct electrostatic precipitator; Journal of Electrostatics 54;2002,p.129-147.

[8] Lawless P. A.; Particle charging bounds, symmetry relations, and an analytic charging rate model for the continuum regime; Journal of Aerosol Sciences; 27; 1996; p. 191-215

[9] Yamamoto T., Velkoff H. R.; Electrohydrodynamics in an electrostatic precipitator; Journal of Fluid Mechanics; volume 108; 1981; p. 1–18.

[10] Lübbert C., Riebel U.; Corona Quenching – Elektroabscheider bei hohen Aerosolkonzentrationen; Chemie Ingenieur Technik; Volume 83; issue 4; 2011; p. 525-534.

[11] Marquard A.,Meyer J., Kasper G.; Influence of corona quenching on charging and collection of nanoparticles; presented at the IX. International conference of electrostatic precipitation; A31-32 series; Kruger Gate,South Africa;2004; Available on homepage of ISESP: http://www.isesp.org

[12] Adachi M., Kousaka Y.,Okuyama K.; Unipolar and bipolar diffusion charging of ultrafine aerosol particles; Journal of aerosol sciences; Volume 16; issue 2; 1985; p. 109-123.

[13] Almeida P. G. C., Benilov M. S., Naidis G. V.; Calculation of ion mobilities by means of the two-temperature displaced-distribution theory; Journal of Physics D: Applied Physics; Volume 35; 2002; p. 1577–1584.

[14] Soldati A., Casal M., Andreussi P., Banerjee S.; Lagrangian simulation of turbulent particle dispersion in electrostatic precipitators; A.I.Ch.E. Journal, Volume 43; 1997; p. 1403–1413.

[15] Schiller, L., Naumann, A.; A Drag Coefficient Correlation. VDI Zeitschrift, 77; 1933; p. 318–320.

[16] Gallimberti I.; Recent advancements in the physical modeling of electrostatic precipitators; Journal of Electrostatics 43; 1998; p. 219-247.

[17] Gallimberti I., Bacchiega G., Bondiou-Clergerie A., Lalande P.; Fundamental processes in long air gap discharges; *C. R.* Physique; 3; 2002; p. 1-25

[18] Lakeh R. B., Molki M.; Patterns of airflow in circular tubes caused by corona jet with concentric and eccentric wire electrodes; Journal of fluids engineering; volume 132; 2010; p. 081201-1 – 081201-10